bioRxiv preprint doi: https://doi.org/10.1101/312876; this version posted July 4, 2018. The copyright holder for this preprint (which was not certified by peer review) is the author/funder, who has granted bioRxiv a license to display the preprint in perpetuity. It is made available under aCC-BY-NC-ND 4.0 International license.

1 # The hydrolase LpqI primes mycobacterial peptidoglycan
2 recycling

3 Patrick J. Moynihan[1]*, Ian T. Cadby[1], Natacha Veerapen[1], Monika Jankute[1], Marialuisa
4 Crosatti[2], Galina V. Mukamolova[2], Andrew L. Lovering[1] and Gurdyal S. Besra[1]
5 **Affiliations:**
6 [1]Institute of Microbiology and Infection
7 School of Biological Sciences
8 University of Birmingham
9 Birmingham, UK, B15 2TT
10
11 [2]Department of Infection, Immunity and Inflammation, University of Leicester, Leicester,
12 LE1 9HN, UK
13
14 *To whom correspondence should be addressed:
15 Patrick J. Moynihan, Ph.D.,
16 Institute of Microbiology and Infection
17 School of Biological Sciences
18 University of Birmingham
19 Birmingham, UK, B15 2TT
20 email: p.j.moynihan@bham.ac.uk
21

bioRxiv preprint doi: https://doi.org/10.1101/312876; this version posted July 4, 2018. The copyright holder for this preprint (which was not certified by peer review) is the author/funder, who has granted bioRxiv a license to display the preprint in perpetuity. It is made available under aCC-BY-NC-ND 4.0 International license.

22 # Abstract

23 Growth and division by most bacteria requires remodeling and cleavage of their cell
24 wall. A byproduct of this process is the generation of free peptidoglycan (PG) fragments
25 known as muropeptides. These muropeptides are recycled in many model organisms, where
26 the bacteria can harness their unique nature as a signal for cell wall damage. These molecules
27 also serve as important signals for hosts where binding to specific receptors reports on the
28 presence of intracellular bacteria. Despite this critical role for muropeptides, it has long been
29 thought that pathogenic mycobacteria such as *Mycobacterium tuberculosis* do not recycle
30 their PG. Herein we show for the first time that *M. tuberculosis* and *Mycobacterium bovis*
31 BCG are able to recycle components of their PG. We demonstrate that the core-mycobacterial
32 gene *lpqI*, encodes an authentic NagZ β-*N*-acetylglucosaminidase and that it is essential for
33 PG-derived amino sugar recycling *via* an unusual pathway. By characterizing an *M. bovis*
34 BCG strain lacking *lpqI* we are also able to show that stem-peptide recycling proceeds
35 independent of amino sugar recovery and loss of *lpqI* leads to antimicrobial resistance *in*
36 *vitro*. Together these data provide a critical first step in understanding how mycobacteria
37 recycle their peptidoglycan.

38

bioRxiv preprint doi: https://doi.org/10.1101/312876; this version posted July 4, 2018. The copyright holder for this preprint (which was not certified by peer review) is the author/funder, who has granted bioRxiv a license to display the preprint in perpetuity. It is made available under aCC-BY-NC-ND 4.0 International license.

39 The cell wall of *M. tuberculosis* is built upon a foundation of peptidoglycan (PG). The
40 remainder of this structure is formed by the modification of muramic acid residues with an
41 arabinogalactan polymer that is in turn esterified by mycolic acids[1]. This waxy coating
42 contributes to drug resistance in *M. tuberculosis*, but is also the target of several
43 mycobacteria-specific antibiotics[1]. The challenge of multi- and extensively-drug resistant *M.*
44 *tuberculosis* has not adequately been met by drug discovery efforts, however recent reports
45 suggest that β-lactams are effective at treating these drug-resistant infections[2-4]. Despite their
46 therapeutic promise, we know relatively little about the turn-over of PG in mycobacteria,
47 which is the eventual target of β-lactam antibiotics.

48 For most bacteria maintenance of a PG sacculus is an essential aspect of life. PG is a
49 heteropolymer comprised of glycan chains with a repeating disaccharide motif of *N*-
50 acetylglucosamine β1→4 *N*-acetylmuramic acid (Glc*N*Ac-Mur*N*Ac) which are then cross-
51 linked to one another *via* short peptides attached to the C-3 D-lactyl moiety of Mur*N*Ac
52 (Figure 1a). The integrity of this macromolecule must be maintained under most growth
53 conditions and its rupture leads to lysis and cell death[5]. As a result of this essentiality, it is
54 vital that cells are able to withstand their own internal turgor pressure and still be able to
55 cleave the cell wall to allow for division, growth and the insertion of macromolecular
56 structures such as secretion systems[5]. Throughout this process, the activity of lytic enzymes or
57 through the attack of host agents like lysozyme, the sacculus is cleaved with the resulting
58 generation of small PG fragments[6].

59 In Gram-positive bacteria muropeptides are typically released from the cell wall
60 through the action of lysozyme-like hydrolytic enzymes, whereas in Gram-negative bacteria,
61 lytic transglycosylases generate 1,6-anhydroMur*N*Ac products[7,8]. These metabolites have
62 been shown to be important in many aspects of host-pathogen interactions. For example,
63 tracheal cytotoxin produced by *Bordetella pertussis* is the product of lytic transglycosylases[9].
64 Release of a similar molecule has also been shown to be involved in tissue damage during

bioRxiv preprint doi: https://doi.org/10.1101/312876; this version posted July 4, 2018. The copyright holder for this preprint (which was not certified by peer review) is the author/funder, who has granted bioRxiv a license to display the preprint in perpetuity. It is made available under aCC-BY-NC-ND 4.0 International license.

65 *Neisseria gonorrhoeae* infection and in the closure of the light-organ of the bobtail squid[10,11].
66 In many organisms, soluble PG acts as a potent immune stimulator once sensed by NOD
67 receptors and other pattern recognition receptors[12].

68 Aside from host organisms, PG metabolites are also important signaling molecules for
69 the bacteria themselves. Recycling of PG has been studied in great detail in a small number of
70 organisms including *Escherichia coli, Pseudomonas aeruginosa* and *Bacillus subtilis* among
71 others[13]. The recycling pathway typically involves the step-wise degradation of the polymer
72 into its monomeric constituents, monosaccharides and amino acids (Figure 1b). Despite
73 common biochemical steps, compartmentalization of these steps tends to be organism
74 specific[7]. The resulting monosaccharides are eventually phosphorylated and Mur*N*Ac-6-
75 phosphate is converted into glucosamine-6-phosphate through the activities of cytoplasmic
76 MurQ and NagA enzymes (Figure 1b). At the same time, the stem peptides are degraded to
77 smaller components and typically shunted back into PG biogenesis. Growth on Mur*N*Ac as a
78 sole carbon-source has never been demonstrated for a bacterium that lacks MurQ.
79 Furthermore, recycling of Mur*N*Ac in a bacterium that lacks MurQ has only been described in
80 *Pseudomonas putida*, and many bacteria, including mycobacteria, are not thought to recycle
81 their PG at all[14].

82 In the present study we sought to determine if mycobacteria are capable of recycling
83 their PG and if so, what impact this has on the bacterium. We for the first time reveal that
84 these bacteria do indeed possess the biochemical capacity to recycle PG elements and
85 determined the molecular basis of Mur*N*Ac recovery. Our data indicate that loss of a key
86 recycling enzyme, LpqI, leads to increased antibiotic and lysozyme resistance.

87 Materials and methods

88 **Bacterial strains and growth conditions:**

bioRxiv preprint doi: https://doi.org/10.1101/312876; this version posted July 4, 2018. The copyright holder for this preprint (which was not certified by peer review) is the author/funder, who has granted bioRxiv a license to display the preprint in perpetuity. It is made available under aCC-BY-NC-ND 4.0 International license.

89 Unless stated otherwise all chemicals and reagents were purchased from Sigma
90 Aldrich. *M. bovis* BCG (Pasteur) and related mutants were maintained on Middlebrook 7H10
91 agar or 7H9 broth supplemented with 10% OADC enrichment and 0.05% Tween 80. Where
92 appropriate kanamycin or hygromycin was added at 25 or 50 $\mu g \bullet mL^{-1}$, respectively.
93 *Mycobacterium smegmatis* mc^2155 was maintained on Tryptic Soy Broth or Tryptic Soy Agar
94 where appropriate. For growth on defined carbon sources, strains were cultivated in Sauton's
95 minimal medium containing per 1 L, 4 g asparagine, 2 g citric acid, 0.5 g K_2HPO_4, 0.5 g
96 $MgSO_4$ * 7 H_2O and 0.05 g ferric ammonium citrate, 0.05% tyloxopol and 5 mM of each
97 carbon source unless stated otherwise[15]. *Escherichia coli* strains were grown in lysogeny
98 broth and supplemented with kanamycin at 50 $\mu g \bullet mL^{-1}$ or hygromycin at 150 $\mu g \bullet mL^{-1}$ where
99 appropriate.

100 **Cloning and purification of Rv0237**

101 Rv0237 was amplified from *M. tuberculosis* H37Rv genomic DNA using standard
102 PCR conditions with the Rv0237SUMOF and Rv0237SUMOR primers and cloned into the T-
103 A site of the Champion pET-SUMO expression plasmid (Invitrogen) according to the
104 manufacturers specifications (all primers are found in Table S2). For production of Rv0237 1
105 L of *E. coli* BL21 [pRv0237] grown in Terrific Broth to an OD_{600} of 0.6, chilled to 20 °C and
106 induced with 1 mM IPTG and grown for a further 18 h before being collected by
107 centrifugation**.** Cells were resuspended in 25 mM Tris-HCl, 300 mM NaCl, 10 mM imidazole
108 pH 7.8 and lysed *via* three passages through a French pressure cell. The protein was purified
109 using standard IMAC procedures with washes of lysis buffer, lysis buffer including 50 mM
110 imidazole and finally eluted with 500 mM imidazole in lysis buffer. Eluted protein was
111 dialysed exhaustively against 25 mM Bis-Tris, 100 mM NaCl pH 7.8 in the presence of
112 recombinant Ulp1 protease which specifically cleaves the His_6-SUMO tag. Digested protein
113 was passed through a second IMAC column (1 mL HisTrap FF, GE Healthcare) and the flow-

bioRxiv preprint doi: https://doi.org/10.1101/312876; this version posted July 4, 2018. The copyright holder for this preprint (which was not certified by peer review) is the author/funder, who has granted bioRxiv a license to display the preprint in perpetuity. It is made available under aCC-BY-NC-ND 4.0 International license.

114 through fraction was found to contain pure, un-tagged Rv0237. Purified protein was dialysed
115 into 25 mM Bis-Tris pH 6.5, 100 mM NaCl.

116 **Crystallography**

117 Prior to crystallization, LpqI was concentrated to 20 mg•mL^{-1} in 25 mM Bis-Tris pH
118 7.5, 100 mM NaCl. LpqI crystals were grown by the sitting-drop vapour diffusion method by
119 mixing an equal volume of protein solution with 1.1 M sodium malonate, 0.1M HEPES, 0.5%
120 w/v Jeffamine ED-2001 (pH 7.0). Crystals were cryo-protected with a saturated solution of
121 sodium malonate and flash -ooled in liquid nitrogen. X-ray data was collected at the Diamond
122 Light Source, Oxford. Data were processed using XiaII and file manipulations were
123 performed using the CCP4 suite of programs. The structure was phased by molecular
124 replacement using the unpublished *M. smegmatis* LpqI structure (PDB: 4YYF) using the
125 program PHASER. The structure was subsequently auto-built in PHENIX and the remaining
126 parts were built in COOT with further refinement using PHENIX and PDB-REDO.

127 **Kinetic characterisation of Rv0237**

128 Purified Rv0237 was evaluated for glycoside hydrolase activity using a variety of
129 substrates. As an initial screening assay, Rv0237 was incubated at 1 μM with either 4-
130 methylumbeliferyl or *p*-nitrophenyl derivatives of a variety of sugars as listed in Figure 4a in
131 Bis-Tris pH 7.5, 100 mM NaCl at 37 °C. The release of *p*-nitrophenol was followed by
132 change in absorbance at 420 nm while production of 4-menthylumbelliferone was monitored
133 by fluorescence as above in a BMG Polarstar spectrophotometer. Kinetic characterisation of
134 Rv0237 was conducted using varying concentrations of 4MU-Glc*N*Ac. The raw data were
135 compared to standards of 4-methylumbelliferone. All data were analysed using GraphPad
136 Prism 7.

137 To evaluate the ability of the enzyme to degrade fragments derived from PG, *M.*
138 *smegmatis* PG was digested with mutanolysin and soluble fragments were prepared and

bioRxiv preprint doi: https://doi.org/10.1101/312876; this version posted July 4, 2018. The copyright holder for this preprint (which was not certified by peer review) is the author/funder, who has granted bioRxiv a license to display the preprint in perpetuity. It is made available under aCC-BY-NC-ND 4.0 International license.

139 quantified as above. Reactions including 1 µM Rv0237, 0.5 mM PG fragments in 25 mM
140 ammonium acetate buffer pH 6.5 were incubated for 18h at 37 °C. In parallel reactions were
141 carried out using *p*NP-Glc*N*Ac in order to monitor enzyme activity visually. The reactions
142 were then evaluated by TLC (Silica 60 F_{254}, Merck, Germany) using a mobile phase
143 consisting of 1-butanol, methanol, ammonium hydroxide and water at a ratio of 5:6:4:1. TLCs
144 were stained with α-naphthol and developed by charring.

145 **Mutant generation**

146 To generate the Δ*lpqI* strain we used specialized transduction according to established
147 protocols[16]. A recombinant *lpqI* knockout phage was designed to replace the chromosomal
148 *lpqI* gene using homologous flanking regions to *lpqI* with a the *sacB* gene and a hygromycin
149 resistance cassette in-between using the LL-Rv0237, LR-Rv0237, RR-Rv0237 and RL-
150 Rv0237 primers. The resulting phage was transduced into *M. bovis* BCG and transductants
151 were selected on 7H10-agar plates containing 75 $\mu g \bullet mL^{-1}$ hygromycin. The mutant was
152 verified by PCR and phenotypically with 4MU-Glc*N*Ac where loss of *lpqI* was expected to
153 abolish turn-over of this fluorescent substrate. The complemented strain was generated by
154 incorporating the *lpqI* gene and 150 bp 5' to the start codon containing the promoter sequence
155 into the promoter-less integrative mycobacterial shuttle vector pMV306 using primers
156 Rv0237CompF and Rv0237CompR to generate the resulting pMV306-*lpqI* plasmid[17]. This
157 was electroporated into *M. bovis* BCG Δ*lpqI* and transformants were selected on 7H10 agar
158 containing hygromycin and kanamycin. The complemented mutant was verified
159 phenotypically with 4MU-Glc*N*Ac. A control strain was also generated using the empty
160 pMV306 vector using the same protocols.

161 **Antimicrobial testing**

162 Mid-exponential cultures of *M. bovis* BCG and derivative strains were diluted to
163 OD_{600} = 0.1 in fresh 7H9 media. 100 µL of this culture was added to a 96-well plate with the

bioRxiv preprint doi: https://doi.org/10.1101/312876; this version posted July 4, 2018. The copyright holder for this preprint (which was not certified by peer review) is the author/funder, who has granted bioRxiv a license to display the preprint in perpetuity. It is made available under aCC-BY-NC-ND 4.0 International license.

164 addition of 1 μL of antibiotic/lysozyme to achieve the desired final concentration as indicated.
165 These were incubated for 7 days at 37 °C at which point 30 μL of 0.02% w/v resazurin and
166 12.5 μL of 20% Tween 80 v/v was added to the culture. This was incubated over-night at 37
167 °C and the production of resorufin was determined by fluorescence (Ex. 530 nm, Em. 590
168 nm) using a BMG Polarstar plate reader.

169 **Rapid purification of mycobacterial cell wall**

170 Rapid purification of cell wall from small cultures was carried out using a modified
171 phenol extraction protocol[18]. Mycobacterial cells were grown to mid-exponential phase and
172 collected by centrifugation. These were washed with cold phosphate-buffered saline (PBS)
173 and resuspended in PBS and the cells were lysed in a Percellys Evolution Bead Beater at
174 5,000 rpm for 3 min. The lysate was then transferred to glass culture tubes to which 2 mL of
175 98% phenol was added and vortexed for 1 min. This was heated for 1h at 70 °C, allowed to
176 cool and the insoluble material was collected by centrifugation at 3,220 x *g*. The aqueous
177 phase was removed and 4 mL of methanol was added. This was vortexed and centrifuged
178 again. Finally, the pellet was washed 3 times with methanol and once with water before being
179 frozen or used for subsequent enzymatic treatment.

180 **Large-scale purification of PG**

181 Purification of PG from *M. smegmatis* was achieved following established protocols[19].
182 Six-liters of *M. smegmatis* were grown to mid-exponential phase (OD_{600} = ~0.6) at which
183 point they were harvested by centrifugation, resuspended in a minimal volume of PBS and
184 lysed by sonication. The resulting lysate was brought to 4% SDS and boiled under reflux for 3
185 h. The insoluble material was collected by centrifugation and washed with water until the
186 SDS was completely removed (at least 7 washes) to yield mycolyl-arabinogalactan-
187 peptidoglycan (mAGP). The mAGP was incubated for 4 days in 0.5% KOH in methanol at 37
188 °C before being washed three times with methanol. The mycolic acids were extracted with 3

bioRxiv preprint doi: https://doi.org/10.1101/312876; this version posted July 4, 2018. The copyright holder for this preprint (which was not certified by peer review) is the author/funder, who has granted bioRxiv a license to display the preprint in perpetuity. It is made available under aCC-BY-NC-ND 4.0 International license.

189 washes of diethyl ether. The phosphodiester linking the AG-PG complex was cleaved using
190 0.2 M H_2SO_4 and the PG was separated from the solubilized AG by centrifugation prior to
191 neutralization with $NaCO_3$ and washed with water 3 times. The insoluble PG pellet was
192 sequentially digested with α-amylase (100 μg•mL^{-1}), DNase (10 μg•mL^{-1}) and RNase (5
193 μg•mL^{-1}) for 8h before proteinase K (100 μg•mL^{-1}) digestion overnight at 37 °C. The PG
194 pellet was resuspended in a minimal volume of 1% SDS and boiled under reflux for 3 h
195 before the SDS was removed by centrifugation and washing with water (at least 7 times). The
196 resulting material was lyophilized and stored at -20 °C until it was needed.

197 Digestion of cell wall material with mutanolysin was carried out overnight at 37 °C in
198 20 mM ammonium acetate buffer (pH 6.0) with continuous mixing. Following digestion,
199 solubilised muropeptides were isolated using graphitized carbon solid-phase-extraction
200 cartridges as previously described[20]. Purified fractions were evaporated to dryness and the
201 concentration of reducing sugars in the pool of soluble muropeptides was assessed using the
202 3-methyl-2-benzothiazolinone hydrazone (MBTH) assay[21].

203 **Synthesis of 4MU-D-lactate**

204 Instead of the 2- or 3- step protocols published for the synthesis of 4MU-D-lactate previously,
205 we used a simplified one step method[22,23]. 1.5 g of (s)-(-)-bromopropionic acid was added to 1
206 g of 4-methylumbelliferone stirring in 40 mL anhydrous dimethylformamide and 0.75 g
207 Cs_2CO_3. This was stirred at room temperature over-night and the product was extracted three
208 times with water/ethyl-acetate and the organic phase was dried over sodium sufate. The
209 organic phase was then filtered and evaporated to dryness. The product was subsequently
210 purified using silica chromatography and was dried as a crystalline white solid.

211 **Turn-over of 4MU reporter compounds by *M. bovis* BCG**

212 To test turn-over of 4MU-Glc*N*Ac or 4MU-D-lactate by whole cells, 100 μL of a mid-
213 exponential culture (OD_{600} = 0.6) was added to a sterile 96 well plate in Sauton's minimal

bioRxiv preprint doi: https://doi.org/10.1101/312876; this version posted July 4, 2018. The copyright holder for this preprint (which was not certified by peer review) is the author/funder, who has granted bioRxiv a license to display the preprint in perpetuity. It is made available under aCC-BY-NC-ND 4.0 International license.

214 media supplemented with 0.05% Tween and 1% glycerol in addition to 1 mM 4MU-D-lactate
215 or 4MU-Glc*N*Ac. Similar controls lacking cells or the reporter compound were included as
216 well. This was incubated at 37 °C and mixed at 300 r.p.m. Each day the fluorescence of the
217 sample was read on a BMC PolarStar microplate reader (Ex. 355 nm; Em 460 nm) with a
218 constant gain setting.

219 **Turn-over of *M. bovis* BCG PG *in vitro***

220 Cultures of *M. bovis* BCG wild-type, Δ*lpqI*, and Δ*lpqI*::*lpqI* were grown to an OD_{600}
221 of 0.6 in the presence of 10 μCi ^{3}H *meso*-diaminopimelic acid (DAP), at which point they
222 were collected by centrifugation, washed 3 times with sterile media and diluted to 0.01 in
223 fresh culture flasks. Periodically a sample of 0.5 mL was taken, and the cells were collected
224 by centrifugation. The spent medium was mixed with 10 mL scinitilation fluid and counted
225 using a liquid scintillation counter. The cell pellet was re-suspended in 10% SDS, boiled for
226 20 min, and centrifuged again. The cell-wall material was then resuspended in 1 mL
227 scintillation fluid and the material was counted in a liquid scintillation counter. The counts of
228 the cell wall and the media were added together to give total ^{3}H DAP in each culture and the
229 data is presented as a percentage of that total. During the course of the experiment the OD_{600}
230 of the culture was monitored daily. All measurements are from three biological replicates.

231 Results

232 **Peptidoglycan Recycling Genes in *Mycobacteria***

233 The genome of *M tuberculosis* encodes many lytic enzymes, including at least five
234 Resuscitation Promoting Factors (Rpfs) and greater than 10 peptidases and amidases in
235 addition to penicillin binding proteins with potential lytic activities[24]. The Rpfs are most
236 likely lytic transglycosylases with the product of RpfB having been recently confirmed as a
237 GlcNAc-1,6-anhydroMurNAc disaccharide[25]. While *M. tuberculosis* does appear to encode at

bioRxiv preprint doi: https://doi.org/10.1101/312876; this version posted July 4, 2018. The copyright holder for this preprint (which was not certified by peer review) is the author/funder, who has granted bioRxiv a license to display the preprint in perpetuity. It is made available under aCC-BY-NC-ND 4.0 International license.

238 least one lysozyme, Rv2525, its activity has not been demonstrated[26]. A recent comparative
239 study of PG-active enzymes in mycobacteria indicated that while significant differences exist,
240 enzymes that can likely degrade all of the major covalent linkages of PG are encoded in the
241 genomes of all mycobacteria[24]. The products of most of these enzymes have not been
242 experimentally demonstrated, however their conservation underscores the importance of PG-
243 remodeling during growth and division of mycobacteria.

244 Most autolytic enzymes produce small PG-metabolites (muropeptides), indicating that
245 mycobacteria should generate these molecules during the course of normal growth. Indeed,
246 soluble PG fragment release has been observed for both *M. smegmatis* and *M. tuberculosis in*
247 *vitro*[18,27]. Given the slow release of PG fragments by mycobacteria, we evaluated the presence
248 of known PG-recycling systems in the genome of several corynebacterial species (Table
249 S1)[14,28]. BLAST analysis of the *Corynebacterium glutamicum, M. tuberculosis,*
250 *Mycobacterium leprae* and *Mycobacterium bovis* BCG genomes indicates that they lack genes
251 related to any known muropeptide import proteins, PG-metabolite phosphorylation systems,
252 and *murQ*. The only sugar-kinase orthologs identified in the genome have previously been
253 characterized as glucose-kinases although they have not been directly tested for amino sugar-
254 phosphotransferase activity[29]. This contrasts sharply with *M. smegmatis* for which an
255 apparently complete "classical" muropeptide recovery system exists, making it a poor model
256 for the PG metabolism of *M. tuberculosis* (Table S1). Taken together, the available data
257 indicates that *M. tuberculosis* and almost all other mycobacteria lack most of the known PG-
258 recycling genes from other bacteria, with only two conserved genes potentially associated
259 with PG-recycling, (*nagA* – Rv3332, *nagZ* – Rv0237).

260 **Biochemical and structural characterisation of LpqI**

261 In previously characterized PG-recycling systems free amino sugars are produced by
262 NagZ, which belongs to the CAZy glycoside hydrolase family 3 (GH3)[30]. This family is a

bioRxiv preprint doi: https://doi.org/10.1101/312876; this version posted July 4, 2018. The copyright holder for this preprint (which was not certified by peer review) is the author/funder, who has granted bioRxiv a license to display the preprint in perpetuity. It is made available under aCC-BY-NC-ND 4.0 International license.

263 large group of enzymes which have hydrolytic and phosphorylytic activity and remove β-
264 linked sugars from proteins and polysaccharides[31,32]. The β-*N*-acetylglucosaminidase sub-
265 family including all known NagZ enzymes utilize a conserved Asp-His catalytic dyad which
266 has been well characterized[33,34]. A BLAST search of the *M. tuberculosis* H37Rv genome
267 revealed only one NagZ ortholog, which was previously named LpqI in light of its
268 identification as a lipoprotein including an appropriately positioned lipobox at the N-terminus
269 of the protein[35]. As a lipoprotein LpqI is expected to be found attached to the external face of
270 the cytoplasmic membrane, which is consistent with proteomics results[35]. LpqI has also been
271 identified as a likely mannosylated glycoprotein in a proteomics screen using ConA
272 chromatography[36]. The *lpqI* gene is found in all mycobacteria with sequenced genomes
273 including *M. leprae* which has a substantially reduced genome indicating that it is involved in
274 a conserved process across all mycobacteria (Table S1, Figure S1).

275 Given the absence of other PG-recycling associated genes, we sought to identify the
276 function of LpqI. While LpqI bears significant sequence similarity to known β-*N*-
277 acetylglucosaminidases, recent studies have demonstrated that divergent activities for this
278 sub-family of enzymes are possible[32]. These activities included the ability to release sugars
279 other than Glc*N*Ac from reporter substrates and apparent phosphorolytic activity. To test this,
280 we cloned, expressed and purified the LpqI protein from *M. tuberculosis* H37Rv using an N-
281 terminal His_6-SUMO tag which was subsequently cleaved from the protein. We first
282 determined if the protein was in fact a β-*N*-acetylglucosaminidase by testing its activity on a
283 variety of substrates including many sugars that would be found in the cell wall of
284 mycobacteria. Using convenient reporter sugars we assessed the ability for the enzyme to
285 release *p*-nitrophenolate or 4-methylumbeliferone from conjugated arabinose, galactose,
286 galactosamine, arabinofuranose, glucose, mannose, mannosamine, glucosamine and *N*-
287 acetylglucosamine (Figure 2a). While not exhaustive, this set of sugars covers most major
288 modifications to the cell wall including the AG itself, *O*-mannose modifications of proteins,

bioRxiv preprint doi: https://doi.org/10.1101/312876; this version posted July 4, 2018. The copyright holder for this preprint (which was not certified by peer review) is the author/funder, who has granted bioRxiv a license to display the preprint in perpetuity. It is made available under aCC-BY-NC-ND 4.0 International license.

289 Gal*N* modification of arabinan, the rhamnose-linker sugar of AG and the Glc*N*Ac and Glc*N*
290 found in PG. The only detectable activity for LpqI was with Glc*N*Ac-containing substrates.
291 Critically, in mycobacteria this sugar is limited to the backbone of PG and a small amount in
292 the linker unit (Mur*N*Ac-6-P-Rha-Glc*N*Ac-galactan) between PG and arabinogalactan. The
293 Michaelis-Menten constants ($k_{cat} = 2.8 \times 10^{-2} \pm 0.04 \times 10^{-2}$ •s^{-1} and $K_m = 106 \pm 5$ μM) of LpqI
294 using 4MU-Glc*N*Ac as a substrate were found to be similar to other NagZ enzymes using this
295 substrate (Figure 2b)[33]. In a similar assay we were also able to show that LpqI releases
296 Glc*N*Ac from soluble PG fragments (Figure 2c). While hydrolytic activity has been reported
297 for most NagZ-type enzymes, a recent report suggested that β-*N*-acetylglucosaminidases from
298 the GH3 family are in fact phosphorylases[32]. Another GH3 β-*N*-acetylglucosaminidase was
299 recently reported to lack this activity, suggesting that it may not be a general property of the
300 family[37]. We tested the activity of the enzyme under the same conditions as reported
301 previously for Nag3 from *Celulomonas fimi* and found that there was no detectable difference
302 with our observed hydrolytic activity. The product of the reaction also co-migrated with
303 Glc*N*Ac on TLCs and not Glc*N*Ac-1-P (Figure S2).

304 To further confirm its function and validate its role in PG-recycling we solved the 1.96
305 Å X-ray crystal structure of LpqI (PDB code: 6GFV; Figure S1, Table S3). LpqI consists of a
306 single TIM-barrel domain similar to cytoplasmic Gram-negative orthologs but lacks the C-
307 terminal domain associated with extracellular NagZ enzymes from some Gram-positive
308 bacteria (Figure S3). Alignment of LpqI with the NagZ/Glc*N*Ac/1,6-anhydroMur*N*Ac
309 complex from *Pseudomonas aeruginosa* ($NagZ_{Pa}$; PDB:5G3R) or NagZ from *Bacillus subtilis*
310 (PDB:4GYJ) resulted in a root-mean-square deviation of 0.96 Å and 1.01 Å respectively
311 (Figure S3). Superposition of the post-cleavage $NagZ_{Pa}$ complex with LpqI indicates that the
312 appropriate coordinating residues for Mur*N*Ac or 1,6-anhydroMur*N*Ac recognition are intact
313 in LpqI, supporting its role in PG-recycling (Figure 2d) [38].

314 **LpqI-catalysed utilisation of peptidoglycan components by mycobacteria**

bioRxiv preprint doi: https://doi.org/10.1101/312876; this version posted July 4, 2018. The copyright holder for this preprint (which was not certified by peer review) is the author/funder, who has granted bioRxiv a license to display the preprint in perpetuity. It is made available under aCC-BY-NC-ND 4.0 International license.

315 Having confirmed the *in vitro* activity of LpqI, we sought to determine the fate of its
316 reaction products, Mur*N*Ac and Glc*N*Ac, in growing *M. bovis* BCG. Prior research has shown
317 that most mycobacteria are unable to use Glc*N*Ac as a sole carbon source, with *M. smegmatis*
318 being one of the notable exceptions[39]. Furthermore, amino acids including L-Ala, L-Glu, and
319 L-Asp have previously been shown to serve as nitrogen sources for *M. tuberculosis* H37Rv[40].
320 To our knowledge, recycling of Glc*N*Ac or Mur*N*Ac has not been reported, nor has recycling
321 been tested for soluble PG fragments. To evaluate this, *M. bovis* BCG was cultured in
322 minimal media supplemented with glycerol (1% v/v) or Mur*N*Ac (0.2% w/v) in Sauton's
323 minimal media with constant aeration. As observed in Figure 3a, *M. bovis* BCG was able to
324 grow using Mur*N*Ac as a sole carbon source. To confirm that this was not a phenotype
325 specific to *M. bovis* BCG we also evaluated the ability of *M. tuberculosis* H37Rv to grow on
326 the same carbon sources with identical results (Figure 3b). Intriguingly growth on Mur*N*Ac in
327 broth was heavily dependent on the aeration of the culture. In contrast, growth on glycerol
328 was unaffected by this change (Figure 3c). To further evaluate the potential for mycobacteria
329 to take up Glc*N*Ac but use it for other purposes other than central metabolism, we tested the
330 ability of *M. bovis* BCG to incorporate ^{14}C Glc*N*Ac into whole cells. Under different growth
331 conditions (rich medium, carbon-poor medium, aerated cultures, static cultures) we were
332 unable to detect significant amounts of Glc*N*Ac being taken up by *M. bovis* BCG. In all cases
333 the c.p.m. of the label in whole-cells was less than or equal to unlabeled controls. We
334 conclude from these data that pathogenic mycobacteria are able to utilise Mur*N*Ac, but not
335 Glc*N*Ac in an O_2-dependent fashion.

336 **Mechanism of Mur*N*Ac metabolism**

337 Given its structural similarity to Glc*N*Ac, the ability of *M. tuberculosis* and *M. bovis*
338 BCG to grow on Mur*N*Ac was surprising and so we evaluated the biochemical processing
339 steps associated with Mur*N*Ac utilization. Mur*N*Ac is a combination of Glc*N*Ac and D-lactate
340 joined by an ether linkage. This suggests that the bacterium is either using the Glc*N*Ac moiety

bioRxiv preprint doi: https://doi.org/10.1101/312876; this version posted July 4, 2018. The copyright holder for this preprint (which was not certified by peer review) is the author/funder, who has granted bioRxiv a license to display the preprint in perpetuity. It is made available under aCC-BY-NC-ND 4.0 International license.

341 for glycolysis, or shunting the lactate derived from Mur*N*Ac into the TCA cycle. We tested
342 this by inhibiting glycolysis with 2-deoxyglucose (2DG) in cultures grown using Mur*N*Ac,
343 glucose and glycerol as sole carbon sources (Figure S4). These data suggested that the
344 pathway of Mur*N*Ac utilization did not require glycolysis and indicated that the lactate moiety
345 of Mur*N*Ac, was instead most likely serving as a carbon source. Consistent with this, when
346 used as a sole carbon source, growth on L-lactate and Mur*N*Ac was O_2 dependent while D-
347 lactate was better utilized under static, 5% CO_2 culture conditions, where Mur*N*Ac could not
348 be used as a carbon source (Figure 3c).

349 These data allow us to hypothesize a mechanism by which *M. bovis* BCG metabolises
350 Mur*N*Ac. Given that metabolism of L-lactate and Mur*N*Ac are O_2-dependent, we anticipate
351 that use of Mur*N*Ac follows cleavage of the D-lactate from Mur*N*Ac *via* an inverting
352 mechanism to produce L-lactate and Glc*N*Ac. In this case, the O_2-dependency on Mur*N*Ac
353 metabolism is likely the result of an O_2-dependent lactate monooxygenase. Consistent with
354 this, two O_2-dependent L-lactate monooxygenases have been identified in *M. tuberculosis*
355 (Rv0694, Rv1872c)[41]. Given the unusual nature of Mur*N*Ac, generation of free lactate by the
356 bacterium would require the activity of a specific lactyl-etherase. To test for the presence of
357 this activity in whole cells, we synthesized a 4MU-D-lactate derivative to serve as a reporter-
358 analog of Mur*N*Ac (Figure S5). Consistent with the presence of a lactyl etherase, cultures of
359 *M. bovis* BCG were able to release 4MU from this compound during the course of growth
360 (Figure 3d). Together these data support a model where mycobacteria cleave the lactyl-moiety
361 from Mur*N*Ac by an as-yet unidentified enzyme and utilise the product of that reaction as a
362 carbon source under aerated conditions.

363 **LpqI-dependent uptake of PG metabolites by mycobacteria**

364 While our data strongly support metabolism of Mur*N*Ac by *M. bovis* BCG, we wanted
365 to confirm the role of LpqI in mycobacterial PG-recycling. To do this we constructed a

bioRxiv preprint doi: https://doi.org/10.1101/312876; this version posted July 4, 2018. The copyright holder for this preprint (which was not certified by peer review) is the author/funder, who has granted bioRxiv a license to display the preprint in perpetuity. It is made available under aCC-BY-NC-ND 4.0 International license.

366 mutant strain of *M. bovis* BCG lacking *lpqI* using specialized transduction[16]. To validate that
367 LpqI is the only β-*N*-acetylglucosaminidase produced by *M. bovis* BCG, we used a whole cell
368 β-*N*-acetylglucosaminidase assay. This demonstrated that *M. bovis* BCG Δ*lpqi* is devoid of β-
369 *N*-acetylglucosaminidase activity as the amount of 4MU released is not significantly different
370 from the spontaneous release in sterile media (Figure 4a). This deficiency is complemented by
371 replacement of the *lpqI* gene at a distal chromosomal location under the control of its native
372 promoter (Δ*lpqi*::*lpqI*) and is not complemented by the empty vector (Δ*lpqi*::EV) (Figure 4a).
373 Growth of Δ*lpqi in vitro* is unaltered as compared to the wild-type (Figure 4c). This mutant
374 therefore provided us with an opportunity to probe the role of disaccharide cleavage in
375 mycobacterial PG-recycling.

376 The order in which muropeptides are recycled, and the chemical structure of the
377 recycled material is critical for the immune sensing of the bacterium. To determine the order
378 of PG-recycling steps, we first determined the impact of the loss of *lpqI* on the recycling of
379 cell wall material. To investigate this, we generated radio-labelled muropeptides and tested
380 them in whole-cell uptake assays. Radiolabelled muropeptides had to be generated in *M.*
381 *smegmatis* due to the inability of *M. bovis* BCG to take-up ^{14}C Glc*N*Ac under the conditions
382 we tested. As shown in Figure 4b, the *M. bovis* BCG Δ*lpqI* mutant took up approximately
383 25% less of the labelled PG than the wild-type (3% vs. 4% respectively). This assay was then
384 repeated using PG fragments labelled with ^{3}H-DAP. In this case, the mutant did take up
385 slightly less of the PG than the wild-type, however this difference was not found to be
386 significant using a two-tailed t-test (Figure 4b). To probe this result further, we pre-labelled
387 cells with ^{3}H DAP and monitored the release of the label into the culture media. Supporting
388 the data above, we observed no significant differences between the wild-type and the Δ*lpqI*
389 strain with respect to the amount of label released to the media (Figure 4c). From these
390 experiments we concluded that LpqI is involved in amino sugar recovery but is not required
391 for stem-peptide recycling.

bioRxiv preprint doi: https://doi.org/10.1101/312876; this version posted July 4, 2018. The copyright holder for this preprint (which was not certified by peer review) is the author/funder, who has granted bioRxiv a license to display the preprint in perpetuity. It is made available under aCC-BY-NC-ND 4.0 International license.

392 Given the inability of *M. bovis* BCG to take up radiolabeled Glc*N*Ac, we were unable
393 to repeat this experiment and follow release of the sugar to the media. To test the impact of
394 deleting *lpqI* on amino sugar recycling by the bacterium, we evaluated its ability to grow on
395 Mur*N*Ac, glycerol and PG. The Δ*lpqI* strain was not deficient for growth on Mur*N*Ac or
396 glycerol, however unlike the wild-type strain it was unable to grow on PG as a sole-carbon
397 source (Figure 4d). Together these data indicate that *in vitro lpqI* is required for PG-derived
398 amino-sugar recycling.

399 **Phenotypic characterisation of a Δ*lpqI* mutant**

400 As indicated above, loss of LpqI did not alter the growth rate of the bacterium *in vitro*.
401 However, given that NagZ-like proteins have been found to play a role in β-lactam sensitivity
402 in other bacteria we sought to determine the antibiotic sensitivity of the Δ*lpqI* strain. In
403 contrast to inhibition of *P. aeruginosa* NagZ, deletion of *lpqI* resulted in an increase in
404 survival in the presence of lysozyme and all cell-wall active antibiotics tested (Figure 5a-d)[42].
405 A smaller impact on survival in the presence of the protein synthesis inhibitor
406 chloramphenicol was observed (Figure 5e). This increase in resistance is not due to a change
407 in cell-wall permeability as determined by ethidium bromide uptake (Figure 5f). These data
408 indicate that *lpqI*-dependent amino sugar recycling is important for the expression of
409 antibiotic resistance by mycobacteria *in vitro*.

410 # Discussion

411 In an attempt to develop diagnostic media for the identification of mycobacteria,
412 several groups in the 1960s observed that *M. tuberculosis* and most other mycobacteria could
413 not metabolise Glc*N*Ac as a sole carbon-source[39,40]. This, along with the absence of known
414 PG recycling-associated genes lead to the assumption that PG recycling is absent in
415 pathogenic mycobacteria. Based on our data and the literature, it is clear that not only is *M.*
416 *tuberculosis* able to recycle its PG *via* a novel pathway, it is generating two distinct classes of

bioRxiv preprint doi: https://doi.org/10.1101/312876; this version posted July 4, 2018. The copyright holder for this preprint (which was not certified by peer review) is the author/funder, who has granted bioRxiv a license to display the preprint in perpetuity. It is made available under aCC-BY-NC-ND 4.0 International license.

417 molecules. These are Glc*N*Ac-Mur*N*Ac-peptide, which is sensed by the host, and Glc*N*Ac-
418 Mur*N*Ac which is sensed by the bacterium. While host-sensing of PG is unaffected by the
419 presence of Glc*N*Ac on NOD-stimulatory molecules, our data indicate that LpqI acts as a
420 regulator for Glc*N*Ac-Mur*N*Ac levels by cleaving disaccharides and allowing the break-down
421 of Mur*N*Ac. In other bacteria cell wall damage can trigger various stress responses, and so it
422 is likely that a build-up of Glc*N*Ac-Mur*N*Ac disaccharides may trigger a stress-like response
423 in mycobacteria[43]. Consistent with this, *lpqI* is encoded adjacent to a universal stress response
424 protein in several species of mycobacteria (Figure S5).

425 As a starting point to investigate PG recycling in *M. tuberculosis*, we investigated the
426 core mycobacterial protein, LpqI. Despite the absence of other known PG-recycling proteins,
427 we have shown that LpqI is an authentic β-*N*-acetylglucosaminidase which is able to cleave
428 PG fragments *in vitro*. Consistent with a role in PG-recycling, *M. bovis* BCG Δ*lpqI* is unable
429 to grow on soluble PG as a sole carbon source, while recycling of the stem-peptide is
430 unaltered in this mutant. Together, our data demonstrate that *M. bovis* BCG and *M.*
431 *tuberculosis* remove the stem-peptide from PG-fragments prior to disaccharide cleavage and
432 lactyl-ether removal (Figure 6). The processing of Glc*N*Ac-Mur*N*Ac by LpqI prior to lactyl-
433 ether cleavage is also supported by our LpqI crystal structure in which the lactate-binding
434 residue R67 from the *P. aeruginosa* structure is conserved (LpqI: R130) suggesting that the
435 physiological substrate of this enzyme possesses the lactyl group[38].

436 Our sole-carbon source assays indicate that while the bacteria are unable to metabolise
437 Glc*N*Ac, surprisingly they can use Mur*N*Ac as a sole carbon source (Figure 3). This is despite
438 the fact that they lack an ortholog of the only known lactyl-etherase, MurQ which cleaves an
439 otherwise stable lactyl-ether in the cytoplasm of most model organisms (Figure 1). Our data
440 indicate that rather than using the Glc*N*Ac portion of the sugar, the bacteria are cleaving the
441 lactyl-ether and metabolising the liberated lactate. During our study we found that *M. bovis*
442 BCG was only able to grow on Mur*N*Ac under aerated conditions. This was also found to be

bioRxiv preprint doi: https://doi.org/10.1101/312876; this version posted July 4, 2018. The copyright holder for this preprint (which was not certified by peer review) is the author/funder, who has granted bioRxiv a license to display the preprint in perpetuity. It is made available under aCC-BY-NC-ND 4.0 International license.

443 the case for L- but not D-lactate which served as a much better carbon source under O_2
444 limiting conditions. As Mur*N*Ac is a combination of D-lactate and Glc*N*Ac, we can predict
445 that the lactyl etherase acting on Mur*N*Ac is proceeding *via* an inverting mechanism. The
446 presence of a specific lactyl-etherase is supported by the turnover of a 4MU-D-lactate reporter
447 compound by *M. bovis* BCG. The O_2 dependence of this growth is intriguing as N-
448 glycolylation is also an O_2-dependent activity, suggesting significant alterations to PG
449 metabolism in hypoxic vs. aerobically growing mycobacteria[44]. Consistent with this
450 observation, expression of *lpqI* is upregulated 2-fold during re-aeration after re-activation
451 from non-replicating persistence in the Wayne hypoxia model[45].

452 The fate of Glc*N*Ac in this pathway remains unclear, although our data and prior
453 observations suggest that the bacteria do not re-use this sugar. This is surprising given the
454 conservation of the *nagA* (Rv3332) gene in mycobacteria, however it is possible that an
455 alternative pathway exists which involves intermediates not generated under the conditions
456 we have tested. This is hinted at with our ^{14}C-labelled muropeptides where incorporation of
457 the labelled-Glc*N*Ac is not expected given the lack of Glc*N*Ac utilisation by the cells. During
458 the production of radio-labelled PG in *M. smegmatis*, a portion of the Glc*N*Ac will have been
459 used by the bacterium to generate Mur*N*Ac rather than strict shunting of Glc*N*Ac into UDP-
460 Glc*N*Ac for cell wall biosynthesis. The subsequent removal of the lactyl-ether from this ^{14}C-
461 Mur*N*Ac by *M. bovis* BCG would then follow steps and intermediates we do not yet fully
462 understand. Indeed, bacterial etherases comprise a diverse number of mechanisms and
463 potential reaction products and so a product other than free Glc*N*Ac is entirely possible[46]. We
464 are currently trying to identify and characterise the enzyme responsible for the observed
465 lactyl-etherase activity.

466 In conclusion, we have identified for the first time a PG recovery pathway in
467 pathogenic mycobacteria. We have shown that this occurs in a step-wise fashion by removing
468 stem-peptide from PG and subsequently cleaving the PG-disaccharide and finally releasing

bioRxiv preprint doi: https://doi.org/10.1101/312876; this version posted July 4, 2018. The copyright holder for this preprint (which was not certified by peer review) is the author/funder, who has granted bioRxiv a license to display the preprint in perpetuity. It is made available under aCC-BY-NC-ND 4.0 International license.

469 the D-lactate from free Mur*N*Ac. Finally, we have shown that recycling of PG by these
470 bacteria is important for lysozyme and antibiotic resistance.

471 **Acknowledgements**

472 We wish to thank Sudagar S. Gurcha and Albel Singh for technical assistance. P.J.M. wishes
473 to acknowledge support in the form of a Future Leader Fellowship from the UK
474 Biotechnology and Biological Sciences Research Council (BB/N011945/1). G.V.M. would
475 like to acknowledge funding from UK Biotechnology and Biological Sciences Research
476 Council (BB/P001513/1). A.L.L. acknowledges funding from UK Biotechnology and
477 Biological Sciences Research Council (BB/J015229/1). M.S. would like to acknowledge
478 funding as an Associate FCT-investigator. G.S.B would like to acknowledge support in the
479 form of a Personal Research Chair from Mr James Bardrick and the UK Medical Research
480 Council (grant MR/K012118/1).
481
482
483
484
485
486 **Author Contributions**

487 Conceived of the study: P.J.M. Conceived and designed the experiments: P.J.M., G.V.M.,
488 M.S., A.L.L., G.S.B. Performed the experiments: P.J.M., A.R.M., I.T.C, N.V., M.J., M.C.
489 Analysed the data: P.J.M., A.R.M., I.T.C, N.V., M.C. G.V.M., M.S., A.L.L., G.S.B. Wrote
490 and edited the paper: P.J.M, G.V.M., M.S., A.L.L., G.S.B.

491

bioRxiv preprint doi: https://doi.org/10.1101/312876; this version posted July 4, 2018. The copyright holder for this preprint (which was not certified by peer review) is the author/funder, who has granted bioRxiv a license to display the preprint in perpetuity. It is made available under aCC-BY-NC-ND 4.0 International license.

492 # Figures and Tables

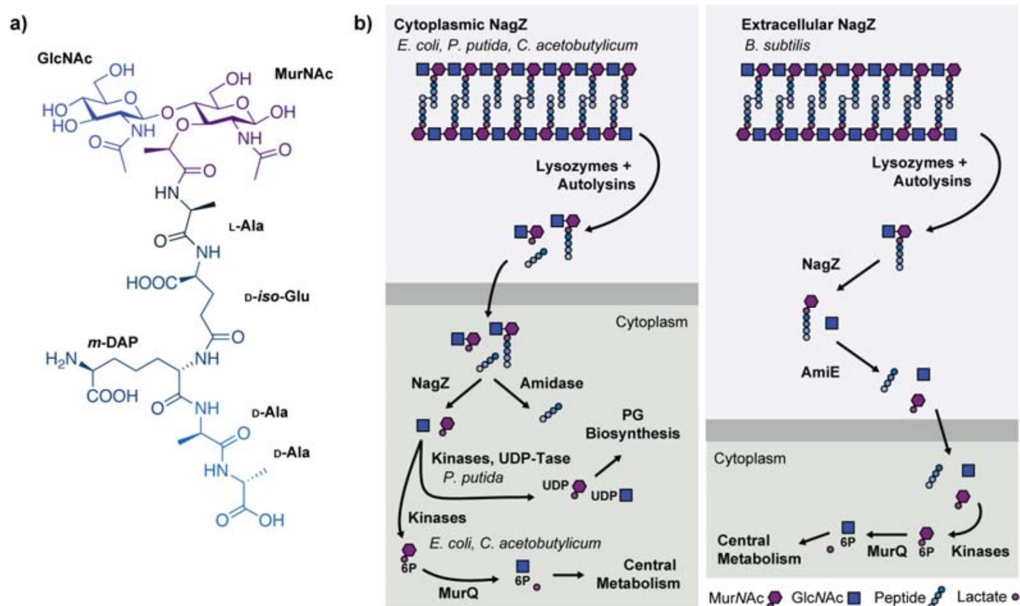

493
494
495 **Figure 1. Overview of PG-recycling. a)** The basic building block of PG is Glc*N*Ac-
496 Mur*N*Ac-pentapeptide. Enzymes produced by the bacterium or the host are able to cleave
497 every major linkage in PG. **b)** The PG recycling machinery is variable with respect to the
498 localisation of NagZ and the subsequent conversion to Glc*N*Ac-1P or UDP-Glc*N*Ac/Mur*N*Ac.
499 All known Mur*N*Ac recovery systems that sustain bacterial growth (as opposed to strictly
500 recycling e.g. *P. putida*) terminate at MurQ in the cytoplasm.
501

bioRxiv preprint doi: https://doi.org/10.1101/312876; this version posted July 4, 2018. The copyright holder for this preprint (which was not certified by peer review) is the author/funder, who has granted bioRxiv a license to display the preprint in perpetuity. It is made available under aCC-BY-NC-ND 4.0 International license.

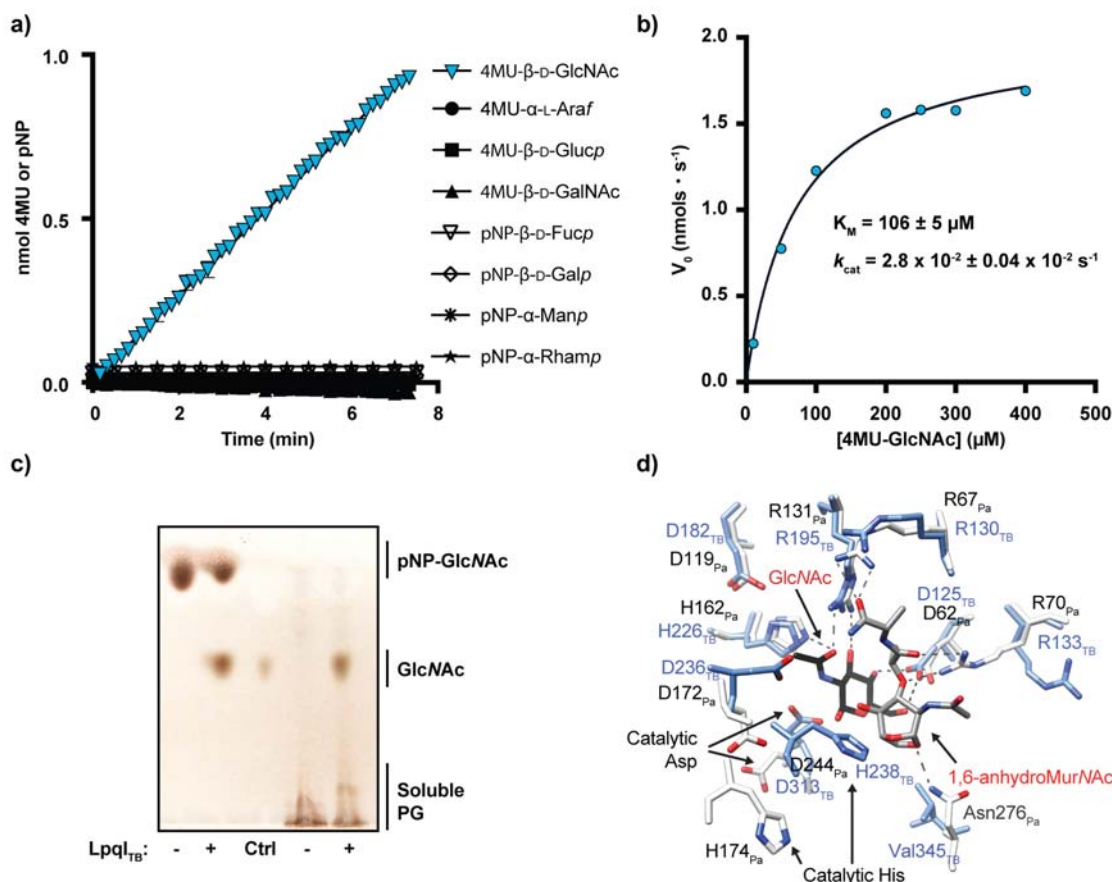

502
503 **Figure 2. LpqI is an authentic NagZ-type enzyme. a)** Reactions including 1 μM LpqI and
504 the indicated chromogenic substrates at 1 mM were incubated at 37 °C and release of pNP or
505 4MU was followed by absorbance or fluorescence respectively. **b)** LpqI was incubated with
506 increasing concentrations of 4MU-Glc*N*Ac. The rate of 4MU release was plotted and the
507 curve fit with the Michaelis-Menton equation using GraphPad Prism 7.0. (n = 3) **c)** LpqI is
508 able to release Glc*N*Ac from soluble muropeptides derived from *M. smegmatis* mc^2155 PG. **d)**
509 The active site of LpqI is highly conserved as evidenced by the nearly identical positioning of
510 key binding residues observed in the Glc*N*Ac, 1,6-anhydroMur*N*Ac complex with $NagZ_{Pa}$
511 (PDB: 5G3R) with an overall RMSD of 1.01 Å.
512
513
514
515
516

bioRxiv preprint doi: https://doi.org/10.1101/312876; this version posted July 4, 2018. The copyright holder for this preprint (which was not certified by peer review) is the author/funder, who has granted bioRxiv a license to display the preprint in perpetuity. It is made available under aCC-BY-NC-ND 4.0 International license.

517
518

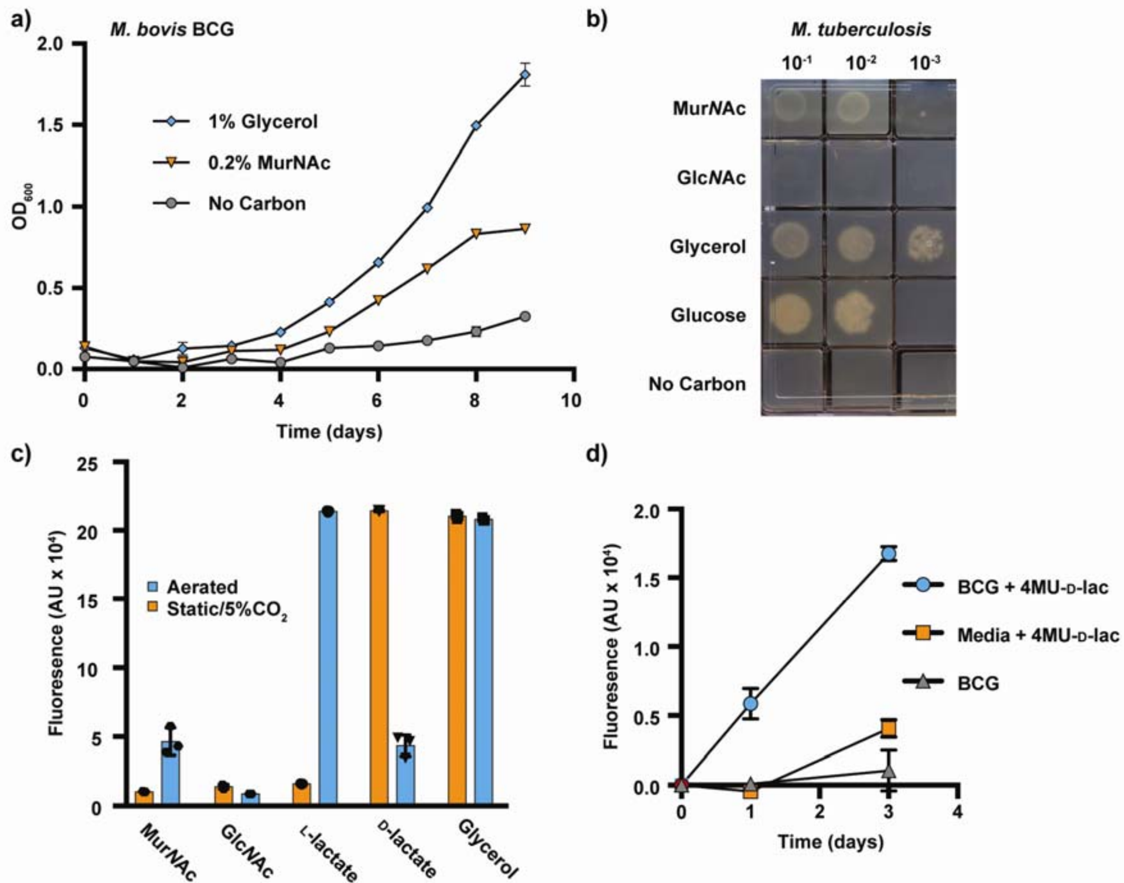

519
520 **Figure 3. *M. tuberculosis* and *M. bovis* BCG are able to recycle Mur*N*Ac. a)** *M. bovis*
521 BCG WT was inoculated at a starting OD_{600} of 0.1 in minimal media containing glycerol and
522 tyloxopol, Mur*N*Ac or no carbon and growth was monitored daily by taking OD_{600} readings at
523 the indicated concentrations (n = 3). **b)** *M. tuberculosis* H37Rv was washed and then serially
524 diluted into fresh carbon-free minimal media. 10 µL of each dilution was spotted onto
525 Sauton's agar containing the indicated carbon sources at 5 mM. **c)** Growth of *M. bovis* BCG
526 on 5 mM Mur*N*Ac, Glc*N*Ac, L-lactate, D-lactate, and glycerol was evaluated in aerated or
527 static 5% CO_2 cultures using a resazurin assay (n = 3). **d)** Mid-exponential *M. bovis* BCG was
528 grown in minimal media with 5 mM glycerol including 1 mM 4MU-D-lactate with constant
529 agitation. At the indicated times the 4MU fluorescence of the samples was determined (n = 3).
530

bioRxiv preprint doi: https://doi.org/10.1101/312876; this version posted July 4, 2018. The copyright holder for this preprint (which was not certified by peer review) is the author/funder, who has granted bioRxiv a license to display the preprint in perpetuity. It is made available under aCC-BY-NC-ND 4.0 International license.

531

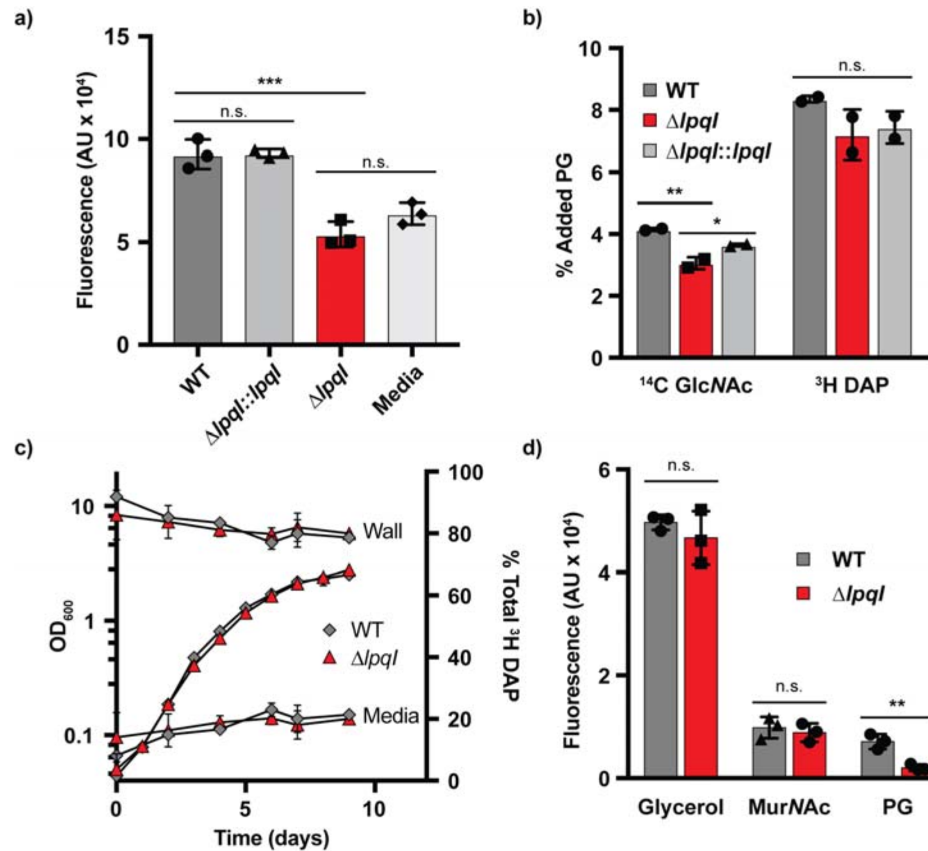

532
533 **Figure 4. *M. bovis* BCG is able to recycle PG. a)** The same strains were incubated with 1
534 mM 4MU-Glc*N*Ac in minimal media. After 3 days the fluorescence of the cultures were
535 measured (n = 3). **b)** *M. bovis* BCG WT, Δ*lpqI* and Δ*lpqI*::*lpqI* were incubated with 30,000
536 CPM of ^{14}C Glc*N*Ac-labelled muropeptides or 100, 000 CPM of ^{3}H DAP-labelled
537 muropeptides for 10 days after which the cell wall material was isolated and subjected to
538 liquid scintillation counting (n = 2). **c)** *M. bovis* BCG WT and Δ*lpqI* were simultaneously
539 evaluated for release of cell wall peptides and growth (n = 3). **d)** The same strains were
540 evaluated for their growth using glycerol, Mur*N*Ac and PG as sole carbon sources using a
541 resazurin assay (n = 3; *** = $p < 0.001$; ** = $p < 0.005$). Statistical significance determined
542 using a two-tailed t-test.
543

bioRxiv preprint doi: https://doi.org/10.1101/312876; this version posted July 4, 2018. The copyright holder for this preprint (which was not certified by peer review) is the author/funder, who has granted bioRxiv a license to display the preprint in perpetuity. It is made available under aCC-BY-NC-ND 4.0 International license.

544
545
546
547

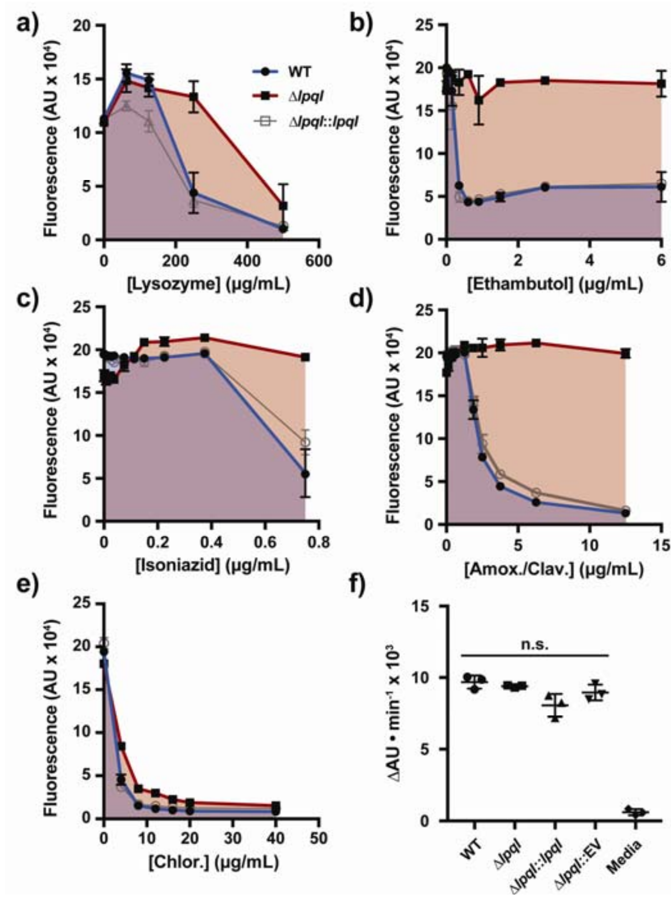

548
549 **Figure 5. Loss of LpqI leads to lysozyme and antibiotic resistance. a-e)** *M. bovis* BCG
550 WT, Δ*lpqI* and Δ*lpqI*::*lpqI* were incubated with increasing concentrations of lysozyme or
551 antibiotics at a starting OD_{600} of 0.1. After 7 days incubation total growth was assessed using
552 a resazurin assay, where total fluorescence correlates with respiration and growth (n = 3). f)
553 *M. bovis* BCG WT, Δ*lpqI* and Δ*lpqI*::*lpqI* and Δ*lpqI*::EV were incubated with EtBr and the
554 rate of EtBr was monitored as an increase in fluorescence. No significant differences were
555 found in pairwise t-tests across all strains (n = 3). Statistical significance determined using a
556 two-tailed t-test.
557
558

bioRxiv preprint doi: https://doi.org/10.1101/312876; this version posted July 4, 2018. The copyright holder for this preprint (which was not certified by peer review) is the author/funder, who has granted bioRxiv a license to display the preprint in perpetuity. It is made available under aCC-BY-NC-ND 4.0 International license.

559
560
561
562
563
564
565
566
567
568
569
570
571
572
573
574
575

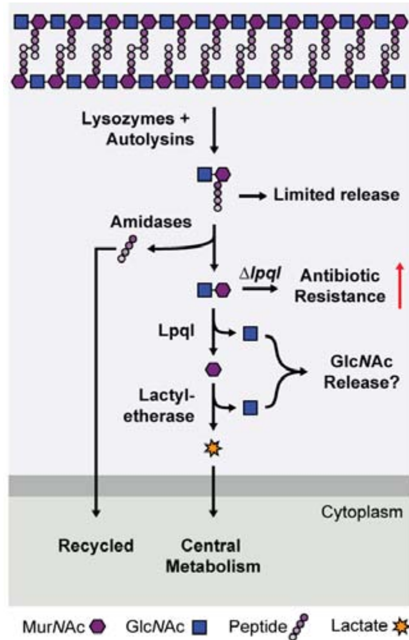

576
577 **Figure 6. Peptidoglycan recovery pathway in pathogenic mycobacteria.** Based on our
578 observations we can propose the following model for PG recycling and recovery in
579 mycobacteria. Cleavage of the cell wall by endogenous autolysins or host-derived lysozyme
580 generates muropeptides. Some of this material undergoes limited release to stimulate the host
581 immune system. The remainder are subsequently degraded by amidases and other peptidases.
582 LpqI then cleaves Glc*N*Ac-Mur*N*Ac, which is followed by D-lactyl-ether cleavage. Lactate
583 can then be used by the cell under aerobic conditions and Glc*N*Ac (or its derivatives) are most
584 likely released. Perturbation of this system by deleting LpqI leads to increased resistance to
585 anti-mycobacterial agents.
586
587
588

589

bioRxiv preprint doi: https://doi.org/10.1101/312876; this version posted July 4, 2018. The copyright holder for this preprint (which was not certified by peer review) is the author/funder, who has granted bioRxiv a license to display the preprint in perpetuity. It is made available under aCC-BY-NC-ND 4.0 International license.

590 # References

591 1. Jankute, M., Cox, J. A. G., Harrison, J. & Besra, G. S. Assembly of the Mycobacterial
592 Cell Wall. *Annu Rev Microbiol* **69,** 405–423 (2015).
593 2. Moynihan, P. J. & Besra, G. S. Colworth prize lecture 2016: exploiting new biological
594 targets from a whole-cell phenotypic screening campaign for TB drug discovery.
595 *Microbiology* **163,** 1385–1388 (2017).
596 3. Diacon, A. H. *et al.* β-Lactams against Tuberculosis--New Trick for an Old Dog? *N.*
597 *Engl. J. Med.* **375,** 393–394 (2016).
598 4. Deshpande, D. *et al.* Ceftazidime-avibactam has potent sterilizing activity against
599 highly drug-resistant tuberculosis. *Science Advances* **3,** e1701102 (2017).
600 5. Santin, Y. G. & Cascales, E. Domestication of a housekeeping transglycosylase for
601 assembly of a Type VI secretion system. *EMBO Rep.* **18,** 138–149 (2017).
602 6. Höltje, J. V. Growth of the stress-bearing and shape-maintaining murein sacculus of
603 *Escherichia coli. Microbiol. Mol. Biol. Rev.* **62,** 181–203 (1998).
604 7. Reith, J. & Mayer, C. Peptidoglycan turnover and recycling in Gram-positive bacteria.
605 *Appl Microbiol Biotechnol* **92,** 1–11 (2011).
606 8. Johnson, J. W., Fisher, J. F. & Mobashery, S. Bacterial cell-wall recycling. *Ann. N. Y.*
607 *Acad. Sci.* **1277,** 54–75 (2013).
608 9. Cookson, B. T., Tyler, A. N. & Goldman, W. E. Primary structure of the
609 peptidoglycan-derived tracheal cytotoxin of *Bordetella pertussis*. *Biochemistry* **28,**
610 1744–1749 (1989).
611 10. Melly, M. & McGee, Z. Ability of monomeric peptidoglycan fragments from *Neisseria*
612 *gonorrhoeae* to damage human fallopian-tube mucosa. *J Infect Dis* (1984).
613 11. Koropatnick, T. A. *et al.* Microbial factor-mediated development in a host-bacterial
614 mutualism. *Science* **306,** 1186–1188 (2004).
615 12. Girardin, S. E. *et al.* NOD1 detects a unique muropeptide from Gram-negative bacterial
616 peptidoglycan. *Science* **300,** 1584–1587 (2003).
617 13. Goodell, E. W. Recycling of murein by *Escherichia coli*. *J Bacteriol* **163,** 305–310
618 (1985).
619 14. Gisin, J., Schneider, A., Nägele, B., Borisova, M. & Mayer, C. A cell wall recycling
620 shortcut that bypasses peptidoglycan *de novo* biosynthesis. *Nat Chem Biol* **9,** 491–493
621 (2013).
622 15. Sauton, B. Sur la nutrition minerale du bacille tuberculeux. *C. R. Acad. Sci* **155,** 860–
623 862 (1912).
624 16. Bardarov, S. *et al.* Specialized transduction: an efficient method for generating marked
625 and unmarked targeted gene disruptions in *Mycobacterium tuberculosis, M. bovis* BCG
626 and *M. smegmatis*. *Microbiology* **148,** 3007–3017 (2002).
627 17. Stover, C. K. *et al.* New use of BCG for recombinant vaccines. *Nature* **351,** 456–460
628 (1991).
629 18. Hancock, I. C., Carman, S., Besra, G. S., Brennan, P. J. & Waite, E. Ligation of
630 arabinogalactan to peptidoglycan in the cell wall of *Mycobacterium smegmatis* requires
631 concomitant synthesis of the two wall polymers. *Microbiology (Reading, Engl)* **148,**
632 3059–3067 (2002).
633 19. Shenderov, K. *et al.* Cord Factor and Peptidoglycan Recapitulate the Th17-Promoting
634 Adjuvant Activity of Mycobacteria through Mincle/CARD9 Signaling and the
635 Inflammasome. *J Immunol* **190,** 5722–5730 (2013).
636 20. Moynihan, P. J. & Clarke, A. J. Substrate Specificity and Kinetic Characterization of
637 Peptidoglycan O-Acetyltransferase B from *Neisseria gonorrhoeae*. *Journal of*
638 *Biological Chemistry* **289,** 16748–16760 (2014).

bioRxiv preprint doi: https://doi.org/10.1101/312876; this version posted July 4, 2018. The copyright holder for this preprint (which was not certified by peer review) is the author/funder, who has granted bioRxiv a license to display the preprint in perpetuity. It is made available under aCC-BY-NC-ND 4.0 International license.

639 21. Jarle Horn, S. & Eijsink, V. G. H. A reliable reducing end assay for chito-
640 oligosaccharides. *Carbohydrate Polymers* **56,** 35–39 (2004).
641 22. Chimichi, S., Boccalini, M., Cravotto, G. & Rosati, O. A new convenient route to
642 enantiopure 2-coumarinyloxypropanals: application to the synthesis of optically active
643 geiparvarin analogues. *Tetrahedron Lett.* **47,** 2405–2408 (2006).
644 23. Chimichi, S. *et al.* Synthesis and biological evaluation of new geiparvarin derivatives.
645 *ChemMedChem* **4,** 769–779 (2009).
646 24. Machowski, E. E., Senzani, S. & Ealand, C. Comparative genomics for mycobacterial
647 peptidoglycan remodelling enzymes reveals extensive genetic multiplicity. *BMC*
648 *Microbiol.* **14,** 75 (2014).
649 25. Nikitushkin, V. D. *et al.* A product of RpfB and RipA joint enzymatic action promotes
650 the resuscitation of dormant mycobacteria. *FEBS J* **282,** 2500–2511 (2015).
651 26. Bellinzoni, M. *et al.* Structural studies suggest a peptidoglycan hydrolase function for
652 the *Mycobacterium tuberculosis* Tat-secreted protein Rv2525c. *J Struct Biol* **188,** 156–
653 164 (2014).
654 27. Takeya, K., Hitsatsune, K. & Nakashima, R. A cell-wall mucopeptide complex
655 obtained from the culture filtrate of tubercle bacilli. *Biochim Biophys Acta* **54,** 595–597
656 (1961).
657 28. Ruscitto, A. *et al.* Identification of a Novel *N*-Acetylmuramic Acid Transporter in
658 *Tannerella forsythia*. *J Bacteriol* **198,** 3119–3125 (2016).
659 29. Marrero, J., Trujillo, C., Rhee, K. Y. & Ehrt, S. Glucose phosphorylation is required
660 for *Mycobacterium tuberculosis* persistence in mice. *PLoS Pathog* **9,** e1003116–
661 e1003116 (2013).
662 30. Cheng, Q., Li, H., Merdek, K. & Park, J. T. Molecular characterization of the beta-*N*-
663 acetylglucosaminidase of *Escherichia coli* and its role in cell wall recycling. *J*
664 *Bacteriol* **182,** 4836–4840 (2000).
665 31. Lombard, V., Golaconda Ramulu, H., Drula, E., Coutinho, P. M. & Henrissat, B. The
666 carbohydrate-active enzymes database (CAZy) in 2013. *Nucleic Acids Res* **42,** D490–
667 D495 (2013).
668 32. Macdonald, S. S., Blaukopf, M. & Withers, S. G. *N*-Acetylglucosaminidases from
669 CAZy Family GH3 Are Really Glycoside Phosphorylases, Thereby Explaining Their
670 Use of Histidine as an Acid/Base Catalyst in Place of Glutamic Acid. *J Biol Chem* **290,**
671 4887–4895 (2015).
672 33. Bacik, J.-P., Whitworth, G. E., Stubbs, K. A., Vocadlo, D. J. & Mark, B. L. Active Site
673 Plasticity within the Glycoside Hydrolase NagZ Underlies a Dynamic Mechanism of
674 Substrate Distortion. *Chem. Biol.* **19,** 1471–1482 (2012).
675 34. Vadlamani, G. *et al.* Conformational flexibility of the glycosidase NagZ allows it to
676 bind structurally diverse inhibitors to suppress β-lactam antibiotic resistance. *Protein*
677 *Sci* **26,** 1161–1170 (2017).
678 35. Målen, H., Pathak, S., Søfteland, T., de Souza, G. A. & Wiker, H. G. Definition of
679 novel cell envelope associated proteins in Triton X-114 extracts of *Mycobacterium*
680 *tuberculosis* H37Rv. *BMC Microbiol.* **10,** 132 (2010).
681 36. González-Zamorano, M. *et al. Mycobacterium tuberculosis* glycoproteomics based on
682 ConA-lectin affinity capture of mannosylated proteins. *J. Proteome Res.* **8,** 721–733
683 (2009).
684 37. Ducatti, D. R. B., Carroll, M. A. & Jakeman, D. L. On the phosphorylase activity of
685 GH3 enzymes: A β-*N*-acetylglucosaminidase from *Herbaspirillum seropedicae* SmR1
686 and a glucosidase from *Saccharopolyspora erythraea*. *Carbohydr Res* **435,** 106–112
687 (2016).
688 38. Acebrón, I. *et al.* Catalytic Cycle of the *N*-Acetylglucosaminidase NagZ from
689 *Pseudomonas aeruginosa*. *J Am Chem Soc* **139,** 6795–6798 (2017).
690 39. Tsukamura, M. Identification of mycobacteria. *Tubercle* **48,** 311–338 (1967).

bioRxiv preprint doi: https://doi.org/10.1101/312876; this version posted July 4, 2018. The copyright holder for this preprint (which was not certified by peer review) is the author/funder, who has granted bioRxiv a license to display the preprint in perpetuity. It is made available under aCC-BY-NC-ND 4.0 International license.

691 40. Bowles, J. A. & Segal, W. Kinetics of Utilization of Organic Compounds in the
692 Growth of *Mycobacterium tuberculosis*. *J Bacteriol* **90,** 157–163 (1965).
693 41. Billig, S. *et al.* Lactate oxidation facilitates growth of *Mycobacterium tuberculosis* in
694 human macrophages. *Scientific Reports* **7,** e10 (2017).
695 42. Zamorano, L. *et al.* NagZ Inactivation Prevents and Reverts β-Lactam Resistance,
696 Driven by AmpD and PBP 4 Mutations, in *Pseudomonas aeruginosa*. *Antimicrob*
697 *Agents Chemother* **54,** 3557–3563 (2010).
698 43. Laubacher, M. E. & Ades, S. E. The Rcs phosphorelay is a cell envelope stress
699 response activated by peptidoglycan stress and contributes to intrinsic antibiotic
700 resistance. *J Bacteriol* **190,** 2065–2074 (2008).
701 44. Raymond, J. B., Mahapatra, S., Crick, D. C. & Martin S Pavelka, J. Identification of
702 the *namH* Gene, Encoding the Hydroxylase Responsible for the *N*-Glycolylation of the
703 Mycobacterial Peptidoglycan. *J Biol Chem* **280,** 326–333 (2005).
704 45. Du, P., Sohaskey, C. D. & Shi, L. Transcriptional and Physiological Changes during
705 *Mycobacterium tuberculosis* Reactivation from Non-replicating Persistence. *Front.*
706 *Microbiol.* **7,** R106 (2016).
707 46. White, G. F., Russell, N. J. & Tidswell, E. C. Bacterial scission of ether bonds.
708 *Microbiol Rev* **60,** 216–232 (1996).
709